Subcellular localization and function of alternatively spliced Noxo1 isoforms

Ueyama, Takehiko
Lekstrom, Kristen
Tsujibe, Satoshi
Saito, Naoaki
Leto, Thomas L.

(Citation)
Free Radical Biology and Medicine,42(2):180-190

(Issue Date)
2007-01

(Resource Type)
journal article

(Version)
Accepted Manuscript

(URL)
https://hdl.handle.net/20.500.14094/90000353

Subcellular localization and function of alternatively spliced Noxo1 isoforms

Takehiko Ueyama†§‡, Kristen Lekstrom†, Satoshi Tsujibe§, Naoaki Saito§,

Thomas L. Leto†‡

† From the Molecular Defenses Section, Laboratory of Host Defenses, National Institute of Allergy and Infectious Diseases, National Institutes of Health, Bethesda 20892, MD, USA, and § Laboratory of Molecular Pharmacology, Biosignal Research Center, Kobe University, Kobe 657-8501, Japan

Running title: Noxo1 Localization & Function

‡Address correspondence to:

Thomas L. Leto

NIH, NIAID, Twinbrook II, Room 203,

12441 Parklawn Dr., Bethesda 20852, MD, USA

Tel: 301-402-5120, Fax: 301-480-1731

E-mail:tleto@nih.gov.

Takehiko Ueyama

Laboratory of Molecular Pharmacology, Biosignal Research Center, Kobe University,

1-1 Rokkodai-cho, Nada-ku, Kobe 657-8501, Japan,

Tel: +81-78-803-5962, Fax: +81-78-803-5971

E-mail: tueyama@kobe-u.ac.jp

This work was supported in part by Grant-in-Aid for Scientific Research, from the 21st Century Center of Excellence (COE) Program and from the Young Scientist, of the Ministry of Education, Culture, Sports, Science and Technology of Japan, and by the Uehara Memorial Foundation of Life Science.

Subcellular localization and function of alternatively spliced Noxo1 isoforms

Abstract Nox organizer 1 (Noxo1), a $p47^{phox}$ homolog, is produced as four isoforms with unique N-terminal PX domains derived by alternative mRNA splicing. We compared the subcellular distribution of these isoforms or their isolated PX domains produced as GFP fusion proteins, as well as their ability to support Nox1 activity in several transfected models. Noxo1α, β, γ, and δ show different subcellular localization patterns, determined by their PX domains. In HEK293 cells, Noxo1β exhibits prominent plasma membrane binding, Noxo1γ shows plasma membrane and nuclear associations, Noxo1α and δ localize primarily on intracellular vesicles or cytoplasmic aggregates, but not the plasma membrane. Nox1 activity correlates with Noxo1 plasma membrane binding in HEK293 cells, since Noxo1β supports the highest activity and Noxo1γ and Noxo1α support moderate or low activities, respectively. In COS-7 cells, where Noxo1α localizes on the plasma membrane, the activities supported by the three isoforms (α, β, and γ) do not differ significantly. The PX domains of β and γ bind the same phospholipids, including phosphatidic acid. These results indicate the variant PX domains are unique determinants of Noxo1 localization and Nox1 function. Finally, the over-expressed Noxo1 isoforms do not affect $p22^{phox}$ localization, although Nox1 is needed to transport $p22^{phox}$ to the plasma membrane.

Introduction

In phagocytic cells, reactive oxygen species (ROS) are produced by NADPH oxidase, an enzyme complex that transports electron across membranes and generates superoxide anion ($O_2^{\cdot -}$) from molecular oxygen. The enzyme is a multi-protein complex assembled from a membrane-spanning flavocytochrome b_{558} heterodimer (composed of $gp91^{phox}$ (Nox2) and $p22^{phox}$) and four cytosolic factors ($p47^{phox}$, $p67^{phox}$, $p40^{phox}$, and Rac) that translocate and associate with the flavocytochrome b_{558} to form an active membrane-bound enzyme [1-3]. Recently, several novel $gp91^{phox}$ (Nox2) homologs have been described in a variety of non-phagocytic cells [4,5]. This new NADPH oxidase or Nox family encompasses 7 homologs of the catalytic, electron carrier component of these enzymes identified in humans: Nox1, Nox2 ($gp91^{phox}$), Nox3, Nox4, Nox5, Duox1, and Duox2.

Two of the closest homologues of the phagocytic oxidase (Nox1 and Nox3) also function as multi-component systems. Nox1 is detected in abundance in the colon and at lower levels in uterus, prostate, and vascular smooth muscle and endothelial cells [6,7]. Nox1 is suggested to function as a host defense oxidase, like Nox2 [8-10]. Based on recent observations in Nox1 knockout mice, Nox1 is also thought to act in the cardiovascular system in the pressor response to Angiotensin II [11,12]. Nox1 expressed alone produces little superoxide, although its activity is significantly enhanced in the presence of two co-factors, Noxo1 and Noxa1, detected in colon

epithelium that are homologous to $p47^{phox}$ and $p67^{phox}$, respectively [13-15] . Noxo1 was proposed to act as a "Nox organizer" based on structural and functional similarities with $p47^{phox}$, which is a multi-modular "adaptor" protein that bridges interactions between the membrane (flavocytochrome b_{558} and lipid) and $p67^{phox}$. Noxa1 was designated as a "Nox activator" based on its homology to $p67^{phox}$, which binds to Rac1 or Rac2 and plays a more direct role in modulating oxidase activity. Recent evidence suggests that Rac1 also regulates Nox1 most likely through GTP-dependent interactions with the Nox activator, Noxa1 [16-19] We showed that the association of Noxa1 with the plasma membrane depends on its interaction with Noxo1 [17]. These structural and functional similarities between the Nox and phox regulators may explain why Noxo1 and Noxa1 can function in partially compensating for $p47^{phox}$ and $p67^{phox}$ in supporting Nox2 activity [8,13-15]. Noxo1, Noxa1, and Rac1 also support Nox3 activity, which appears to function critically in the inner ear [17,20-22]; mice with lesions in either the *NOX3* or *NOXO1* gene have defects in sensing gravity resulting from impaired otoconia formation [23,24]. Nox3 activity can be supported by $p47^{phox}$ and $p67^{phox}$, although mice deficient in $p47^{phox}$ or chronic granulomatous disease patients deficient in either protein show no deficits in balance.

Several groups described structural variants of human Noxo1, which were proposed to result from alternative splicing of mRNA sequences encoding their PX domains [14,15,25,26]. We characterized Noxo1α and showed that it supports Nox1 activity in several transfected cell

models (Genbank™ accession no. AY255768) [14]. Most reports studied Noxo1β (human or mouse), the most common isoform [9,13,15,17,25]. Noxo1β and Noxo1γ isoforms were compared recently for their abilities to support Nox1 and Nox3-based oxidases [26]. Noxo1γ supports lower levels of Nox3 activity than Noxo1β, although both isoforms show similar phospholipid binding specificities. Since PX domains in other proteins were shown to engage in either protein-lipid or protein-protein interactions and they appear to serve in subcellular targeting of several proteins [27,28], we examined the subcellular distribution of spliced Noxo1 isoforms in relation to their ability to support oxidase activity in several Nox1 reconstituted cell models. We show that the PX domains of Noxo1 variants dictate unique subcellular distribution patterns that can, in turn, influence their abilities to support oxidase function.

Materials and Methods

Materials

Mouse monoclonal antibody (Ab) against $p22^{phox}$ (#449) was a kind gift from Drs. Arthur J. Verhoeven and Dirk Roos [29]. Mouse monoclonal Ab against human β-tubulin was from Sigma-Aldrich. Rabbit polyclonal Ab against green fluorescent protein (GFP) and Hoechst 33258 were from Clontech.

Cell Culture

All cell culture reagents were obtained from Invitrogen, unless indicated otherwise. HEK293 cells (ATCC) were maintained in EMEM containing 10% heat-inactivated FBS (Hyclone Laboratories), 1 mM sodium pyruvate, 100 μM nonessential amino acids, and antibiotics (100 units/ml penicillin and 100 μg/ml streptomycin) at 37°C in 5% CO_2. CHO-K1 cells (ATCC) were maintained in Ham's F-12 medium containing 10% heat-inactivated FBS, and antibiotics at 37°C in 5% CO_2. COS-7 cells (ATCC) were maintained in DMEM containing 10% heat-inactivated FBS, and antibiotics at 37°C in 5% CO_2. PANC-1 cells (ATCC) were maintained in DMEM containing 10% heat-inactivated FBS and antibiotics at 37°C in 5% CO_2. MT3 cells (ATCC) were maintained in DMEM/F12 containing 2.5% heat-inactivated FBS and 5% horse serum, and antibiotics at 37°C in 5% CO_2.

Construction of plasmids

The pcDNA3.1 plasmids (Invitrogen) containing the complete coding sequence of human Nox1, $p41^{nox}$ (Noxo1α and Noxo1β), $p51^{nox}$ (Noxa1), and $p22^{phox}$ were described previously [5,8,17]. Human Noxo1γ in pcDNA3.1 and Noxo1δ in pcDNA3.1were made from Noxo1β and Noxo1α using the QuickChange II XL Site-Directed Mutagenesis Kit (Stratagene), respectively. PX domains of Noxo1α (a.a. 1-146), Noxo1β (a.a. 1-147), Noxo1γ (a.a. 1-152), and Noxo1δ (a.a. 1-151) were amplified by PCR and cloned into the Eco*RI* and Bam*HI* sites of pEGFP-N1 (Clontech), and designated Noxo1α(PX)-GFP, Noxo1β(PX)-GFP, Noxo1γ(PX)-GFP, and Noxo1δ(PX)-GFP, respectively. Full-length Noxo1α, Noxo1β, Noxo1γ, and Noxo1δ were amplified by PCR and cloned into the Eco*RI* and Bam*HI* sites of pEGFP-N1 (Clontech), and designated Noxo1α-GFP, Noxo1β-GFP, Noxo1γ-GFP, and Noxo1δ-GFP respectively. We confirmed that Noxo1-GFPs support Nox1 activity in the presence of Noxa1 at levels comparable to unfused, wild-type Noxo1 isoforms (data not shown). All other amino acid mutations [($p22^{phox}$(P156Q), GFP-Noxo1β(R40Q)] were produced using the QuickChange II XL Site-Directed Mutagenesis Kit. All modified expression vectors were sequenced to confirm their identities.

Cell imaging

Cells (HEK293, COS-7, PANC-1, or TM3 cells) were seeded on 35-mm glass bottom dishes (MatTek Chambers) and transfected using FuGENE 6 (Roche Applied Science). Forty to

48 hours after the transfection, cells were fixed using 10% formalin in buffered solution (Sigma-Aldrich). After permeabilization with TBS containing 0.3% Triton X-100 for 10 min, the fixed cells were stained for 2 h at RT using $p22^{phox}$ antibody at 1:200 dilutions (TBS-T with 5% BSA). Secondary antibody-fluor conjugates (anti-mouse Alexa 488 or Alexa 594; 1:2000 dilutions) were applied for 0.5 h at RT. Confocal imaging was performed using a TCS-SP2 ABOS confocal laser scanning fluorescence microscope (63x oil) (Leica Microsystems GmBH).

Immunoblotting

Cells were lysed in homogenizing buffer in the present of protease inhibitors and 1 % Triton X-100 [30] by sonication. The total cell lysates were probed by Western blotting using primary Ab ($p22^{phox}$, 1/1000; GFP, 1/2000; RT for 2 h). Bound antibodies were detected with secondary antibody-HRP conjugates (Jackson ImmunoResearch Laboratories) using the ECL detection system (Amersham Biosciences).

Cell transfections and ROS assays

Cells were seeded in 6-well dishes at 250,000 cells/well (HEK293 cells), 70,000 cells/well (CHO-K1 or COS-7 cells) for 48 h prior to transfection. Transfections were performed in serum-free medium using 6 µl of FuGENE 6 prepared in complexes with plasmid DNAs (total 2µg/well, 0.5 µg of Nox1 (in pcDNA3.1), plus 0.5 µg each of other expression vectors (Noxo1, Noxa1 and $p22^{phox}$(P156Q) in pcDNA3.1) or pcDNA3.1 (control) plasmid), using the

manufacturer's suggested protocol. The cells were fed 5 h post-transfection with complete medium, and were assayed 48 h after transfection. Trypsinized cells (250,000 cells) were assayed for ROS release (with or without 2 μg/ml PMA) by SOD-inhibitable chemiluminescence methods using the Diogenes reagent (National Diagnotics), as described previously [17].

Protein-lipid overlay assay

PCR-amplified PX domains adapted with termination codons from Noxo1α(a.a. 1-146), Noxo1β(a.a. 1-147), and Noxo1γ (a.a. 1-152) were cloned into the Bam*HI* and Eco*RI* sites of pGEX-2T (Amersham Biosciences). All constructs were sequenced to confirm their identities. Protein fused to glutathione S-transferase (GST) were expressed in *Escherichia coli* strain BL21-CodonPlus (DE3)-RIL (Stratagene). When the bacteria reached an OD_{600} of ~0.2, protein expression was induced with 0.1 mM isopropyl β-thioglucopyranoside (Sigma-Aldrich) at 21°C for 16 h, solubulized by 50 mM CHAPS, and purified by glutathione-sepharose-4B (Amersham Biosciences). Protein-lipid overlay assays were performed using PIP Strips™ (Invitrogen), as described previously [31]. Briefly, PIP Strips™ membranes were blocked in 2 % fatty acid-free BSA in TBST buffer (50 mM Tris-HCl, 150 mM NaCl, and 0.1% Tween 20, pH 7.5) for 1 h at RT. The membranes were then incubated for 3 h at RT in the same solution with 20 nM (≈ 0.86 μg/ml of Noxo1, ≈ 0.53 μg/ml of GST) GST-tagged protein. The membranes were washed 5 times for 1 h (each wash) in TBST buffer and then incubated for 1 h with 1/2000 dilution of anti-GST

polyclonal Ab (Santa Cruz Biotechnology). The membranes were washed as before prior to probing for 1 h with 1/10000 dilution of anti-rabbit HRP conjugate (Jackson ImmunoResearch Laboratories). Following washing, the bound protein was detected by ECL detection system.

RT-PCR amplification and identification of Noxo1 isoforms

RT-PCR was performed using the first strand cDNA prepared from colon, testis, liver, and pancreas RNA (Human MTC™ panels I and II; Clontech). For the PCR amplification using Herculase® Enhanced DNA polymerase (Stratagene), 10 μl of the first strand cDNA was denatured for 2 min at 95°C prior to 40 cycles at 95°C for 30 s, 57°C for 30 s, and 72°C for 30 s. The primers used for amplification were 5'-ggcagccctggtgcagatcaagaggc-3' and 5'-cagtcgccagcagcctccgagaatagg-3'. The PCR fragments are subcloned into the Zero Blunt TOPO vector (Invitrogen) and the identities of these PCR fragments were confirmed by DNA sequencing.

Statistic analysis

Data are presented as the percent of the maximally reconstituted oxidase activities observed in the absence of cell stimulation and was expressed as means ± SD (100% was defined with Nox1 + Noxo1β + Noxa1 co-expression in each cell line). Each assay was performed in duplicate and was repeated in at least three independent transfection experiments.

Results

Alternative splicing of Noxo1 and its effects on PX domain structure

Four variants of human Noxo1 have been designated as Noxo1α, β, γ, and δ isoforms that differ within sequences encoding their N-terminal, PX domains. These variants were suggested to result from alternative mRNA splicing of coding sequences within the 5' and 3' boundaries of exon 3 (Fig. 1A and B) [26]. Noxo1α and δ isoforms derive from transcripts lacking a single AAG codon corresponding to lysine 50 of the β and γ isoforms; these variants result from the use of alternative splice acceptor sites (splice site 1) on the 5' boundary of exon 3 (Fig. 1B and C). The γ and δ isoforms contain an additional five amino acids (GQASL), resulting from use of an alternative splice donor site on the 3' end of exon 3 (splice site 2). As noted earlier [26], all splice patterns conform to the GT-AG rule for the boundaries of these splice sites [32] suggesting these structural variants derive from genuine mRNA splicing mechanisms and are not artifacts of reverse transcription or PCR reactions. The conserved murine genomic sequences are compatible with similar alternative splicing mechanisms, and would produce the same sequences variants (Fig. 1B). Furthermore, some GenBank™ cDNA sequences suggest that similar alternative mRNA splicing occurs in the Noxo1 genes from mice and chimpanzees: GenBank™ accession no. BI409553 describes a murine cDNA lacking the lysine 50 codon, as in the human α and δ isoforms, while FASTA™ accession no. XP_523481 describes a chimpanzee protein that

contains the "GQASL" motif present in human γ and δ isoforms, suggesting that these conserved sequences serve some common function across species.

The PX domain sequences of the Noxo1 isoforms were aligned with PX domains of other proteins (Fig. 1C). This comparison reveals that lysine 50 in Noxo1β and γ is surrounded by highly conserved sequences in all other PX domains, which have been shown to form α-helices in the three-dimensional structures of $p47^{phox}$, $p40^{phox}$, Vam7p, and phosphoplipase D1 (PLD1) [Fig. 1C, [33-37]]. Thus, the absence of lysine 50 would likely have drastic effects on the overall conformation of the PX domains of the Noxo1 α and δ forms. Indeed, no other PX domains contain deletions comparable to the splice site 1 deletion observed in these two isoforms. In contrast, the extra five residues in γ and δ isoforms (splice site 2) occur within a region that is variable in other PX domains. This insertion aligns within the "PXXP" motif of $p47^{phox}$ and PLD1, which is exposed and can engage in either intramolecular or intermolecular protein-protein interactions [34,38]. Several other proteins contain PX domains that lack this proline-rich motif entirely [27]. Thus, the extra splice site 2 sequence found in Noxo1 γ and δ most likely would not affect the overall conformation of their PX domains, and these isoforms may interact with unique targets that would not bind to α or β forms.

Noxo1α, Noxo1β, Noxo1γ, and Noxo1δ exhibit unique subcellular localization patterns

Noxo1 Localization & Function

To explore functional differences among Noxo1 isoforms, we examined the subcellular localization of the PX domains and full-length Noxo1 isoforms using GFP-tagged molecules expressed in two cell models. Previous work showed that the fusion of GFP to the C-terminus of Noxo1β has no detectable effect on its ability to support Nox1 activity [17]. In the HEK293 cell model, Noxo1α(PX)-GFP and Noxo1α-GFP, as well as Noxo1δ(PX)-GFP and Noxo1δ-GFP are detected primarily within intracellular membrane structures or in large cytoplasmic aggregates, but not on the plasma membrane (Fig. 2A). In contrast, Noxo1β(PX)-GFP and Noxo1β-GFP are localized predominately along the plasma membrane (Fig. 2A). Noxo1γ(PX)-GFP and Noxo1γ-GFP are also localized on the plasma membrane but are most prominently localized in the nucleus; their detection on the plasma membrane is weaker than that of Noxo1β, particularly with Noxo1γ(PX)-GFP (Fig. 2A). In the COS-7 cell model, Noxo1α(PX)-GFP, Noxo1α-GFP show some association with the plasma membrane, as well as with punctuate vesicular structures dispersed throughout the cytoplasm (Fig. 2B). The tendency to form large aggregates is much less than is seen in HEK293 cells, and may reflect differences in efficiencies in which the two lines synthesize or process these proteins. The appearance of full-length and PX domain fusion proteins of Noxo1β and Noxo1γ isoforms is similar along the plasma membrane of COS-7 cells, however, Noxo1γ(PX)-GFP or Noxo1γ-GFP are again detected in the nucleus. Noxo1δ(PX)-GFP or Noxo1δ-GFP are not detected in nuclear sites, as seen with

Noxo1γ(PX)-GFP or Noxo1γ-GFP, either in HEK293 or COS-7 cells (Fig. 2B and C). Furthermore, their detection on the plasma membrane in COS-7 cells is less than that observed with the other isoforms (Fig. 2C). In CHO-K1 cells, the localization patterns of Noxo1(PX)-GFP and Noxo1-GFP proteins are similar to those in HEK293 cells (data not shown). Interestingly, the prominent plasma membrane targeting of Noxo1β-GFP is disrupted by the R40Q mutation; this mutant is detected in small punctuate structure dispersed throughout the cytoplasm and faintly along the plasma membrane (Fig. 2C). These observations indicate that the PX domains are major determinants of the subcellular distribution of Noxo1, since each isoform is targeted to distinct subcellular sites.

Immunoblotting of the four full-length Noxo1-GFP proteins reveals comparable levels of the intact proteins, and no detectable degradation in either transfected model (Fig. 2D). Thus, the large intracellular bodies of GFP-tagged Noxo1α and Noxo1δ (full-length and PX domain) forms most likely reflect aggregation of misfolded α or δ-PX domains, despite the lack of any significant degradation of these proteins.

Functional differences between Noxo1 isoforms in reconstituted Nox1 systems

We examined the ability of Noxo1 isoforms to support the Nox1 system using three transfected cell models (HEK293, COS-7, and CHO-K1). Our studies focused primarily on the

α, β, and γ isoforms, because Noxo1δ shows no distinctive localization pattern; it is similar to Noxo1α, appearing predominantly in cytoplamic aggregates or vesicles. In HEK293 and CHO-K1 cell models, Noxo1β supports the highest Nox1 activity, while Noxo1γ and Noxo1α support moderate or low levels of activity, respectively (Fig. 3A and C). Among the four Noxo1 isoforms, Noxo1δ supports the lowest levels of Nox1 activity in the HEK293 cell model (data not shown). In contrast, Nox1 activity in COS-7 cells is supported at comparable levels by three Noxo1 isoforms (Fig. 3B). A dominant negative effect of $p22^{phox}$(P156Q) is seen with all isoforms expressed; interestingly, this effect is most apparent with the Noxo1α isoform. A PMA enhancing effect on oxidase activity is seen in three cell models, however, the COS-7 cell model shows a higher constitutive component, consistent with Noxo1 plasma membrane binding seen with all three isoforms. Comparison of the absolute levels of Nox1 activity (RLU, normalized by cell number) supported by Noxo1 isoforms shows that COS-7 cells have the highest activity, HEK293 cells have moderate, and CHO-K1 cells have the lowest activity (Fig. 1D). The lower activity in CHO-K1 cells is likely due to the low expression of $p22^{phox}$ compared with HEK293 and COS-7 cells [15,39]. ROS production observed with the transfected wild-type (unfused) Noxo1 isoforms was the same as that observed using GFP-tagged Noxo1 isoforms (data not shown), consistent with earlier work on Noxo1β [17].

Phospholipid binding of Noxo1β and Noxo1γ

To explore further the basis for differences in subcellular localization and function of the Noxo1 isoforms, we examined phopholipid binding of their PX domains using protein-lipid overlay assays. The GST-Noxo1(PX) fusion proteins existed primarily in an insoluble fraction when expressed in *E. coli*. Using CHAPS as a detergent, GST-Noxo1β(PX) and GST-Noxo1γ(PX) were solublized and purified as single bands by glutathione-sepharose affinity chromatography, however, GST-Noxo1α(PX) could not be purified as a single species at the expected molecular weight (Fig. 4A), suggesting that this form may be misfolded and unstable against proteolysis in *E. coli* (Fig. 4A). Thus, binding studies were performed using GST-Noxo1β(PX) and GST-Noxo1γ(PX). Both proteins bind to the monophosphorylated phosphatidylinositol lipids, PtdIns-(3)P, PtdIns-(4)P, and PtdIns-(5)P, and to PtdIns-(3,5)P_2 (Fig. 4B). These results showing that the PX domains of both isoforms have similar phospholipid binding specificities are similar to those reported recently [26], although that study did not detect binding to PtdIns-(3)P. In addition, we detected binding of both GST-Noxo1β(PX) and GST-Noxo1γ(PX) to phosphatidic acid (PA). We observed the same phospholipid binding specificities using PIP Strips™ from another source (Echelon Biosciences; data not shown). GST alone does not bind any of these phospholipids (Fig. 4B).

Tissue-specific expression patterns of Noxo1 isoforms

It has been reported that Noxo1 is expressed predominately in colon, testis, pancreas, and liver using real time PCR [15], thus, we examined the expression patterns of Noxo1 isoforms in these tissues using PCR primers targeted to their entire PX domains. We detected Noxo1 mRNA by RT-PCR in colon, testis, liver, and pancreas, although these products are only weakly detected in pancreas (Fig. 5A). These PCR amplified products were cloned and several were selected of sequence analysis. Each isoform exhibited a unique expression pattern in the tissues examined (Fig. 5B). Noxo1β mRNA is expressed in all tissues and is the predominant isoform in colon, pancreas, and liver. Noxo1γ mRNA is also expressed in all tissues and is the predominant isoform in testis. Both Noxo1α and Noxo1δ are expressed at relatively low frequency; Noxo1δ is detected only in liver. These distinct tissue-specific expression patterns are similar to those reported recently by others [26], although these authors detected a higher frequency of the α form in the colon carcinoma cell-line, T84.

In view of these distinct expression patterns, we examined the localization of Noxo1 isoforms in epithelial cell lines from pancreas (PANC-1) and testis (TM3). All three Noxo1 isoforms are localized on the plasma membrane in both cell types, most efficiently with Noxo1β and Noxo1γ (Fig. 5C). Interestingly, Noxo1α shows a lesser tendency to aggregate in these cells compared with the HEK293 cell model, and is weakly detect on the plasma membrane as

well as other intracellular membranes. Noxo1γ is localized on the plasma membrane and in the nucleus, as seen in HEK293and COS-7 cells.

Plasma membrane targeting of p22^{phox} by Nox1, but not by Noxo1 isoforms

Since Noxo1 is an organizer protein that links Noxa1 to the Nox1 flavocytochrome heterodimer through a direct interaction with p22^{phox}, we examined the subcellular localization of p22^{phox} in relation to Noxo1 in transfected HEK293 cell model. Endogenous p22^{phox} in HEK293 cells has a reticular intracellular and perinuclear staining pattern, which likely reflects its accumulation in the endoplasmic reticulum (ER) (Fig. 6A, left), although no p22^{phox} is detected in the nucleus. Transfected p22^{phox} displays a similar staining pattern (Fig. 6A, middle). As previously described [17], transfection of Nox1 increases detectable levels of endogenous p22^{phox} and results in a dramatic redistribution of endogenous p22^{phox}, resulting in significant accumulation along the plasma membrane (Fig. 6A, right). In contrast, transfection of various Noxo1-GFP isoforms causes no alterations in the endogenous p22^{phox} staining pattern; in particular, there is no plasma membrane or nuclear targeting of endogenous p22^{phox} caused by over-expression of Noxo1β-GFP or Noxo1γ-GFP (Fig. 6B). Furthermore, we did not observe any redistribution or increases in endogenous levels of p22^{phox} following transfection of the wild-type Noxo1 isoforms (data not shown). The increases in p22^{phox} levels caused by

transfection of Nox1, but not Noxo1, is confirmed by Western blotting (Fig. 6C) and is consistent with a recent report showing that cfp-tagged $p22^{phox}$ expression levels were increased by co-transfection with Nox1 [40]. These observations support the hypothesis that Nox1 is stabilized through its heterodimeric association with $p22^{phox}$ and that their transport to the plasma membrane occurs only when the two chains are co-expressed. In contrast, Noxo1 has no apparent role in targeting the $p22^{phox}$ to the membrane. Thus, it appears that the $p22^{phox}$-Nox1 heterodimeric complex, once transported to the plasma membrane, provide a docking site forNoxo1-and Noxa1, resulting in superoxide release into the extracellular environment.

Discussion

Earlier studies have shown that regulation of Nox1 is similar to that of the phagocytic NADPH oxidase (Nox2), in that it requires several supportive co-factors. Nox1 activity depends on at least three cytoplasmic proteins: Noxo1 and Noxa1 (homologs of $p47^{phox}$ and $p67^{phox}$, respectively) and the small GTPase, Rac1 [13-15,17-19,25]. GTP-bound Rac1 appears to regulate Nox1 through its binding partner, Noxa1, which is in turn dependent on Noxo1 to associate with the plasma membrane [17]. This report provides a functional characterization of Noxo1 by comparing the subcellular localization of alternatively spliced PX domain isoforms of Noxo1 (α, β, γ and δ) in relation to their abilities to support Nox1 activity.

Four structural variants of human Noxo1 (α, β, γ, and δ) have been reported that appear to derive from alternative mRNA splicing within two sites of the coding sequence of the PX domain [14,15,26]. PX domains function in subcellular targeting of many intracellular signaling proteins by binding to specific phosphoinositide lipids and other protein partners. In this study, we show that the PX domain of Noxo1 is the most important determinant of Noxo1 isoform localization, since the full-length proteins, or their isolated PX domains, fused to GFP exhibit similar subcellular distribution patterns. In addition, plasma membrane targeting of Noxo1 is the most important correlate of its ability to support Nox1 activity. We observed the following rank order of activities in supporting Nox1 among the Noxo1 isoforms: Noxo1β ≥ Noxo1γ >>

Noxo1α > Noxo1δ. Noxo1β and γ show the most prominent association with the plasma membrane and they support the highest levels of oxidase activity in HEK293 cells. Noxo1α supports Nox1 activity in COS-7 cells much better than in HEK293 cells, which correlates with its more efficient targeting to the plasma membrane of COS-7 cells. All of the isoforms were detected at comparable levels (Fig. 2D), thus differences in their stabilities does not account for their functional differences. Finally, plasma membrane targeting of Noxo1β-GFP is dramatically disrupted with the Noxo1β(R40Q)-GFP mutant (Fig. 2C), which correlates with the lower Nox1 activity supported by this mutant [25]. These observations are consistent with the co-localization of Noxo1β and Nox1 on the plasma membrane of HEK293 cells, which is seen even without cell stimulation [25].

Although the Noxo1 PX domain has a dominant role in plasma membrane targeting, the interaction of Noxo1 with $p22^{phox}$ also clearly contributes to Nox1 function. Noxo1 was shown to bind $p22^{phox}$ *in vitro* through its SH3 domain interaction with proline-rich motif in the C-terminal domain of $p22^{phox}$ [15]. Co-localization of Noxo1-RFP and $p22^{phox}$-GFP on the plasma membrane, to a minor extent, and on the ER, to a greater extent, was observed in HEK293H cells [25]. However, in HEK293 cells both endogenous and exogenous over-expressed $p22^{phox}$ are retained in the ER, and are noy association with the plasma membrane (our current and earlier studies [17]). Furthermore, we showed that expression of Nox1

efficiently targets endogenous p22^{phox} to the plasma membrane [Fig. 6A, [17]], while the expression of various Noxo1 isoforms does not alter the localization of endogenous p22^{phox} (Fig. 6B). The requirement of Nox2-p22^{phox} heterodimer formation for both stabilization and maturation of this complex has been well established [41]. This concept is consistent with our observations showing that expression of Nox1, but not Noxo1, enhances detectable levels of endogenous p22^{phox} (Fig. 6C) and targets endogenous p22^{phox} to the plasma membrane in a heterodimeric complex with Nox1 that is capable of delivering superoxide to the extracellular medium (Fig. 6B). We observe dominant negative effects of mutant p22^{phox}(P156Q) in three Nox1 systems reconstituted with Noxo1 isoforms (α, β, and γ). Interestingly, the effect is most apparent with Noxo1α, which shows the weakest association with the plasma membrane. Thus, both the PX domain-membrane interaction and SH3 domain-p22^{phox} interaction contribute to the interaction of Noxo1 with the membrane and its assembly with the active oxidase complex, although Noxo1 serves no apparent role in localization of the Nox1-p22^{phox} heterodimer. A similar dual interaction with the membrane is well described in the case of p47^{phox}, although both interactions are prevented in the absence of cell stimulation [34,36,42]. Nuclear localization of Nox1 and of p22^{phox} has been reported in transformed human gingival keratinocytes [43] and in human umbilical vein endothelial cells (HUVEC) [44], respectively. Although we could not detect p22^{phox} in the nucleus in HEK293 cells (Fig. 6A and B), it is possible that a nuclear

Nox-p22^{phox} heterodimer expressed in other cell types may be supported by this nuclear-targeted Noxo1 isoform, Noxo1γ. A nuclear-targeted Nox system may be tailored for more effective modulation of redox-responsive genes. Alternatively, Noxo1γ may function as an adaptor protein in other nuclear signaling complexes.

The distinct subcellular targeting of Noxo1α and γ to sites other than the plasma membrane raises interesting questions regarding the structural and functional consequences of alternative splicing of the Noxo1 PX domain sequence. The omission of a single lysine (splice site 1 deletion) in the middle of an otherwise highly conserved amphipathic α-helix (α–1) in Noxo1α or δ would likely disrupt folding of the entire PX domain, since all residues beyond this deletion would be shifted 100 degrees out of register. Consistent with this prediction, the intact form of the Noxo1α PX-GST fusion protein is not stably produced in *E. coli.* The full-length or PX domain-GFP fusion proteins of Noxo1α are unexpectedly stable in transfected mammalian cells, although they show a tendency to aggregate in the cytoplasm of several cell types, suggesting they are misfolded when over-expressed. Noxo1α likely binds to the membrane and supports Nox1 through it interaction with p22^{phox}, independent of a functional PX domain, consistent with its lower Nox1 supporting activity and the effects of the p22^{phox}(P156Q).

In contrast to splice site 1, alternative splicing at splice site 2 likely has little effect on protein folding, since the additional "GQASL" motif, seen in the γ and δ forms, occurs within a

region that is variable (both in length and sequence) and is exposed on the surface of all PX domains (Fig. 1C). In several proteins, this region contains the proline-rich, "PXXP" motif that makes contact with SH3 domains through intramolecular or intermolecular interactions; this polyproline type II helix lies adjacent to the major anionic lipid recognition site that binds phosphatidylinositol lipids. The corresponding Noxo1 sequence contains two prolines, although their sequence positions do not conform to any consensus of SH3 domain binding sequences (either in the presence or absence of the splice site 2 motif). The lipid binding specificities of Noxo1β and γ PX domains are similar (Fig. 4B and [26]), thus the additional splice site 2 sequence (GQASL) in Noxo1γ does not appear to affect lipid binding. It is likely that this peptide targets Noxo1γ to the nucleus. In $p47^{phox}$ the PX domain proline-rich motif was shown to interact with the second SH3 domain within $p47^{phox}$, thereby masking the phosphatidylinositol-binding pocket and preventing this membrane interaction in the absence of cell stimulation and $p47^{phox}$ phosphorylation [34,36]. Thus, the absence of a suitable SH3-binding motif in the PX-domains of all Noxo1 isoforms, in addition to the absence of sequence homologous to the phosphorylated auto-inhibitory of $p47^{phox}$, could explain why these proteins are membrane-bound even without cell stimulation. Nox1 activity is also significantly enhanced by cell stimulation in several transfected models, including NIH3T3, HEK293, CHO-K1, COS-7, T84, HT-29 cells [this study, [9,14,15,17]]. The basis for PMA-stimulated

Nox1 activity remains unclear, since Noxo1 localization on plasma membranes is not altered following cell stimulation (data not shown). Phosphorylation may activate the pre-assembled, membrane-bound Nox1 complex or activate Rac.

The Noxo1 and p47^{phox} PX domains also differ with respect to the phosphatidylinositol lipids they recognize. Critical phosphoinositide binding residues identified in p47^{phox} [36], which are thought to favor binding of PtdIns-(3,4)P_2, are not conserved in any Noxo1 isoform. For example, p47^{phox} residues R43, F44, T45, and R90 coincide with Noxo1β residues S41, W42, D43, and R91 (Fig. 1C). S41 replaces basic residues observed in all other PtdIns-(3)P binding PX domains, while the tryptophan is atypical of the aromatic residues observed at the floor of this binding pocket (invariably tyrosine or phenylalanine). Interestingly, we observed binding of PA to Noxo1β and γ, as was reported previously with p47^{phox}; this was attributed to the existence of a second anionic lipid binding pocket in p47^{phox} [36,45]. PA binding to Noxo1 is likely due to the remarkable structural similarities of Noxo1 within regions identified within this second site of p47^{phox}. The p47^{phox} residues lining this pocket (helix-1 and those preceding the proline-rich motif: H51, K55, R70, P73 and H74) correspond to Noxo1 residues K49, K53, R68, P71, and K72. These striking similarities suggest that PA binding to Noxo1β and Noxo1γ involves a conserved secondary anionic lipid-binding site similar to that mapped in the PX domain of p47^{phox}.

Noxo1 Localization & Function

In addition to the functional differences between Noxo1 isoforms, we confirmed and extended earlier work showing that each isoform has a distinct, tissue-specific expression pattern [18]. Noxo1α and Noxo1δ are expressed in low abundance in colon, testis, liver, and pancreas: Noxo1α, in testis (2/11) and liver (2/11); Noxo1δ, only one clone in liver (1/11). Production of the Noxo1α may be favored in pathological states, since Noxo1α was originally cloned from colon cancer cell line (GeneBank™ accession no. BC015917, IMAGE: 4661469) and was not detected from normal colon cDNA in the present study. Moreover, Noxo1δ may be the least relevant isoform in physiological terms, since it is not detected in normal colon or testis cDNA (Fig. 5B), it is not efficiently targeted to the nucleus or plasma membrane (Fig. 2A and B), and it supports the lowest Nox1 activity of all four isoforms (data not shown). When expressed in pancreatic (PANC-1) or testis (TM3) epithelial cell lines the Noxo1 α, β, and γ isoforms show the same distinctive localization patterns observed in the other transfected models, however Noxo1α is less aggregated and is detected along the plasma membrane. We do not know the relevant oxidase systems expressed in these cells nor could we compare Noxo1 isoform functions in these lines, because of their low transfection efficiency. Noxo1 is also a physiologically relevant partner of Nox3, since lesions in either murine gene result in the same distinctive inner ear phenotype, defective otoconia formation and loss of balance [23,24]. We observed the following rank order of Nox3 activities supported by Noxo1 isoforms in the HEK293 cell model:

Noxo1β > Noxo1γ > Noxo1α, similar to that observed with Nox1 (data not shown). These observations are consistent with previous work showing that Nox3 prefers Noxo1β to Noxo1γ [26]. Noxo1γ is remarkably different from Noxo1β in terms of its cellular localization and expression patterns; Noxo1γ-GFP is detected in the nucleus, as well as the plasma membrane, and is the predominant isoform expressed in testis. Further study is needed to define distinct physiological roles of these isoforms.

Acknowledgements

This work was supported in part by Grant-in-Aid for Scientific Research, from the 21st Century Center of Excellence (COE) Program and from the Young Scientist, of the Ministry of Education, Culture, Sports, Science and Technology of Japan, and by the Uehara Memorial Foundation of Life Science.

Abbeviations used: ROS, reactive oxygen species; Noxo1, Nox organizer 1; Noxa1, Nox activator 1; Ab, antibody; ER, endoplasmic reticulum; GFP, green fluorescence protein; RFP, red fluorescence protein; GST, glutathione S-transferase; PA, phosphatidic acid

References

[1] Leto, T.L. Inflamation: basic principles and clinical correlates. In: Gallin, J.I.;Snyderman, R., eds. The respiratory burst oxidase, Philadelphia: Lippincott Williams & Wilkins; 1999: 769-787.

[2] Babior, B.M. NADPH oxidase. *Curr Opin Immunol* **16:**42-7; 2004.

[3] Quinn, M.T.;Gauss, K.A. Structure and regulation of the neutrophil respiratory burst oxidase: comparison with nonphagocyte oxidases. *J Leukoc Biol* **76:**760-81; 2004.

[4] Lambeth, J.D. NOX enzymes and the biology of reactive oxygen. *Nat Rev Immunol* **4:**181-9; 2004.

[5] Geiszt, M.;Leto, T.L. The Nox Family of NAD(P)H Oxidases: Host Defense and Beyond. *J. Biol. Chem.* **279:**51715-51718; 2004.

[6] Suh, Y.-A.;Arnold, R.S.;Lassegue, B.;Shi, J.;Xu, X.;Sorescu, D.;Chung, A.B.;Griendling, K.K.;Lambeth, J.D. Cell transformation by the superoxide-generating oxidase Mox1. *Nature* **401:**79-82; 1999.

[7] Ago, T.;Kitazono, T.;Kuroda, J.;Kumai, Y.;Kamouchi, M.;Ooboshi, H.;Wakisaka, M.;Kawahara, T.;Rokutan, K.;Ibayashi, S.;Iida, M. NAD(P)H oxidases in rat basilar arterial endothelial cells. *Stroke* **36:**1040-6; 2005.

[8] Geiszt, M.;Lekstrom, K.;Brenner, S.;Hewitt, S.M.;Dana, R.;Malech, H.L.;Leto, T.L. NAD(P)H Oxidase 1, a Product of Differentiated Colon Epithelial Cells, Can Partially Replace Glycoprotein 91^{phox} in the Regulated Production of Superoxide by Phagocytes. *J Immunol* **171:**299-306; 2003.

[9] Kawahara, T.;Kuwano, Y.;Teshima-Kondo, S.;Takeya, R.;Sumimoto, H.;Kishi, K.;Tsunawaki, S.;Hirayama, T.;Rokutan, K. Role of Nicotinamide Adenine Dinucleotide Phosphate Oxidase 1 in Oxidative Burst Response to Toll-Like Receptor 5 Signaling in Large Intestinal Epithelial Cells *J Immunol* **172:**3051-3058; 2004.

[10] Szanto, I.;Rubbia-Brandt, L.;Kiss, P.;Steger, K.;Banfi, B.;Kovari, E.;Herrmann, F.;Hadengue, A.;Krause, K.H. Expression of NOX1, a superoxide-generating NADPH oxidase, in colon cancer and inflammatory bowel disease. *J Pathol* **207:**164-76; 2005.

[11] Matsuno, K.;Yamada, H.;Iwata, K.;Jin, D.;Katsuyama, M.;Matsuki, M.;Takai, S.;Yamanishi, K.;Miyazaki, M.;Matsubara, H.;Yabe-Nishimura, C. Nox1 is involved in angiotensin II-mediated hypertension: a study in Nox1-deficient mice. *Circulation* **112:**2677-85; 2005.

[12] Gavazzi, G.;Banfi, B.;Deffert, C.;Fiette, L.;Schappi, M.;Herrmann, F.;Krause, K.H. Decreased blood pressure in NOX1-deficient mice. *FEBS Lett* **580:**497-504; 2006.

[13] Banfi, B.;Clark, R.A.;Steger, K.;Krause, K.-H. Two Novel Proteins Activate Superoxide

Generation by the NADPH Oxidase NOX1. *J. Biol. Chem.* **278:**3510-3513; 2003.

[14] Geiszt, M.;Lekstrom, K.;Witta, J.;Leto, T.L. Proteins Homologous to p47^{phox} and p67^{phox} Support Superoxide Production by NAD(P)H Oxidase 1 in Colon Epithelial Cells. *J. Biol. Chem.* **278:**20006-20012; 2003.

[15] Takeya, R.;Ueno, N.;Kami, K.;Taura, M.;Kohjima, M.;Izaki, T.;Nunoi, H.;Sumimoto, H. Novel Human Homologues of p47^{phox} and p67^{phox} Participate in Activation of Superoxide-producing NADPH Oxidases. *J. Biol. Chem.* **278:**25234-25246; 2003.

[16] Kawahara, T.;Kohjima, M.;Kuwano, Y.;Mino, H.;Teshima-Kondo, S.;Takeya, R.;Tsunawaki, S.;Wada, A.;Sumimoto, H.;Rokutan, K. Helicobacter pylori lipopolysaccharide activates Rac1 and transcription of NADPH oxidase Nox1 and its organizer NOXO1 in guinea pig gastric mucosal cells. *Am J Physiol Cell Physiol* **288:**C450-457; 2005.

[17] Ueyama, T.;Geiszt, M.;Leto, T.L. Involvement of Rac1 in Activation of Multicomponent Nox1- and Nox3-Based NADPH Oxidases. *Mol. Cell. Biol.* **26:**2160-2174; 2006.

[18] Cheng, G.;Diebold, B.A.;Hughes, Y.;Lambeth, J.D. Nox1-dependent Reactive Oxygen Generation Is Regulated by Rac1. *J Biol Chem* **281:**17718-26; 2006.

[19] Miyano, K.;Ueno, N.;Takeya, R.;Sumimoto, H. Direct involvement of the small GTPase Rac in activation of the superoxide-producing NADPH oxidase Nox1. *J Biol Chem*; 2006.

[20] Cheng, G.;Ritsick, D.;Lambeth, J.D. Nox3 Regulation by NOXO1, p47phox, and p67phox. *J. Biol. Chem.* **279:**34250-34255; 2004.

[21] Banfi, B.;Malgrange, B.;Knisz, J.;Steger, K.;Dubois-Dauphin, M.;Krause, K.-H. NOX3, a Superoxide-generating NADPH Oxidase of the Inner Ear. *J. Biol. Chem.* **279:**46065-46072; 2004.

[22] Ueno, N.;Takeya, R.;Miyano, K.;Kikuchi, H.;Sumimoto, H. The NADPH oxidase Nox3 constitutively produces superoxide in a p22^{phox}-dependent manner: Its regulation by oxidase organizers and activators. *J Biol Chem*; 2005.

[23] Paffenholz, R.;Bergstrom, R.A.;Pasutto, F.;Wabnitz, P.;Munroe, R.J.;Jagla, W.;Heinzmann, U.;Marquardt, A.;Bareiss, A.;Laufs, J.;Russ, A.;Stumm, G.;Schimenti, J.C.;Bergstrom, D.E. Vestibular defects in head-tilt mice result from mutations in Nox3, encoding an NADPH oxidase. *Genes Dev.* **18:**486-491; 2004.

[24] Kiss, P.J.;Knisz, J.;Zhang, Y.;Baltrusaitis, J.;Sigmund, C.D.;Thalmann, R.;Smith, R.J.;Verpy, E.;Banfi, B. Inactivation of NADPH oxidase organizer 1 Results in Severe Imbalance. *Curr Biol* **16:**208-13; 2006.

[25] Cheng, G.;Lambeth, J.D. NOXO1, Regulation of Lipid Binding, Localization, and Activation of Nox1 by the Phox Homology (PX) Domain. *J. Biol. Chem.* **279:**4737-4742; 2004.

Noxo1 Localization & Function

[26] Cheng, G.;Lambeth, J.D. Alternative mRNA splice forms of NOXO1: differential tissue expression and regulation of Nox1 and Nox3. *Gene* **356:**118-26; 2005.

[27] Sato, T.K.;Overduin, M.;Emr, S.D. Location, location, location: membrane targeting directed by PX domains. *Science* **294:**1881-5; 2001.

[28] Ellson, C.D.;Andrews, S.;Stephens, L.R.;Hawkins, P.T. The PX domain: a new phosphoinositide-binding module. *J Cell Sci* **115:**1099-105; 2002.

[29] Verhoeven, A.J.;Bolscher, B.G.;Meerhof, L.J.;van Zwieten, R.;Keijer, J.;Weening, R.S.;Roos, D. Characterization of two monoclonal antibodies against cytochrome b_{558} of human neutrophils. *Blood* **73:**1686-94; 1989.

[30] Nunoi, H.;Rotrosen, D.;Gallin, J.I.;Malech, H.L. Two forms of autosomal chronic granulomatous disease lack distinct neutrophil cytosol factors. *Science* **242:**1298-301; 1988.

[31] Ueyama, T.;Eto, M.;Kami, K.;Tatsuno, T.;Kobayashi, T.;Shirai, Y.;Lennartz, M.R.;Takeya, R.;Sumimoto, H.;Saito, N. Isoform-specific Membrane Targeting Mechanism of Rac During FcγR-mediated Phagocytosis. *J Immunol* **175:**2381-90; 2005.

[32] Mount, S.M. A catalogue of splice junction sequences. *Nucleic Acids Res* **10:**459-72; 1982.

[33] Bravo, J.;Karathanassis, D.;Pacold, C.M.;Pacold, M.E.;Ellson, C.D.;Anderson, K.E.;Butler, P.J.;Lavenir, I.;Perisic, O.;Hawkins, P.T.;Stephens, L.;Williams, R.L. The crystal structure of the PX domain from p40(phox) bound to phosphatidylinositol 3-phosphate. *Mol Cell* **8:**829-39; 2001.

[34] Hiroaki, H.;Ago, T.;Ito, T.;Sumimoto, H.;Kohda, D. Solution structure of the PX domain, a target of the SH3 domain. *Nat Struct Biol* **8:**526-30; 2001.

[35] Lu, J.;Garcia, J.;Dulubova, I.;Sudhof, T.C.;Rizo, J. Solution structure of the Vam7p PX domain. *Biochemistry* **41:**5956-62; 2002.

[36] Karathanassis, D.;Stahelin, R.V.;Bravo, J.;Perisic, O.;Pacold, C.M.;Cho, W.;Williams, R.L. Binding of the PX domain of $p47^{phox}$ to phosphatidylinositol 3,4-bisphosphate and phosphatidic acid is masked by an intramolecular interaction. *Embo J* **21:**5057-68; 2002.

[37] Stahelin, R.V.;Ananthanarayanan, B.;Blatner, N.R.;Singh, S.;Bruzik, K.S.;Murray, D.;Cho, W. Mechanism of membrane binding of the phospholipase D1 PX domain. *J Biol Chem* **279:**54918-26; 2004.

[38] Jang, I.H.;Lee, S.;Park, J.B.;Kim, J.H.;Lee, C.S.;Hur, E.M.;Kim, I.S.;Kim, K.T.;Yagisawa, H.;Suh, P.G.;Ryu, S.H. The direct interaction of phospholipase C-γ 1 with phospholipase D2 is important for epidermal growth factor signaling. *J Biol Chem* **278:**18184-90; 2003.

[39] Biberstine-Kinkade, K.J.;Yu, L.;Stull, N.;LeRoy, B.;Bennett, S.;Cross, A.;Dinauer, M.C. Mutagenesis of $p22^{phox}$ histidine 94. A histidine in this position is not required for

flavocytochrome b_{558} function. *J Biol Chem* **277:**30368-74; 2002.

[40] Ambasta, R.K.;Kumar, P.;Griendling, K.K.;Schmidt, H.H.H.W.;Busse, R.;Brandes, R.P. Direct Interaction of the Novel Nox Proteins with $p22^{phox}$ Is Required for the Formation of a Functionally Active NADPH Oxidase. *J. Biol. Chem.* **279:**45935-45941; 2004.

[41] Yu, L.;Zhen, L.;Dinauer, M.C. Biosynthesis of the phagocyte NADPH oxidase cytochrome b_{558}. Role of heme incorporation and heterodimer formation in maturation and stability of $gp91^{phox}$ and $p22^{phox}$ subunits. *J Biol Chem* **272:**27288-94; 1997.

[42] Ago, T.;Kuribayashi, F.;Hiroaki, H.;Takeya, R.;Ito, T.;Kohda, D.;Sumimoto, H. Phosphorylation of $p47^{phox}$ directs phox homology domain from SH3 domain toward phosphoinositides, leading to phagocyte NADPH oxidase activation. *Proc Natl Acad Sci U S A* **100:**4474-9; 2003.

[43] Chamulitrat, W.;Schmidt, R.;Tomakidi, P.;Stremmel, W.;Chunglok, W.;Kawahara, T.;Rokutan, K. Association of $gp91^{phox}$ homolog Nox1 with anchorage-independent growth and MAP kinase-activation of transformed human keratinocytes. *Oncogene* **22:**6045-53; 2003.

[44] Kuroda, J.;Nakagawa, K.;Yamasaki, T.;Nakamura, K.;Takeya, R.;Kuribayashi, F.;Imajoh-Ohmi, S.;Igarashi, K.;Shibata, Y.;Sueishi, K.;Sumimoto, H. The superoxide-producing NAD(P)H oxidase Nox4 in the nucleus of human vascular endothelial cells. *Genes Cells* **10:**1139-51; 2005.

[45] Stahelin, R.V.;Burian, A.;Bruzik, K.S.;Murray, D.;Cho, W. Membrane binding mechanisms of the PX domains of NADPH oxidase $p40^{phox}$ and $p47^{phox}$. *J Biol Chem* **278:**14469-79; 2003.

Figure Legends

Fig. 1

Alternative splicing of Noxo1 transcripts and its affects on PX domain structure.

A, Schematic of Noxo1 gene organization, showing locations of alternative splice sites on both boundaries of exon 3 (blue and red). Exons are shown as numbered boxes, while introns are represented as thin lines. B, Alignment of human and mouse Noxo1 genomic sequences around exon 3. Capital and bold letters show exonic sequences, while small letters denote intronic sequences. Amino acids encoded by alternative splicing are shown in blue and red at the beginning and end of exon 3, respectively. Arrows and arrowheads indicate alternative splice donor and splice acceptor sites, respectively. C, Alignment of Noxo1 isoform PX domain sequences with those of other PX domains (conserved amino acids shown in pink). Conserved secondary structural elements identified within the three-dimensional structure of $p47^{phox}$ are shown above sequences (α, alpha helix; β, beta sheet)[34,36]. Amino acids resulting from alternative splicing at sites 1 and 2 are shown in blue and red, respectively. Splice site 1 (1) occurs in the middle of conserved α-helix 1, while splice site 2 (2) occurs within a variable sequence that includes a proline-rich motif that interacts with SH3 domains in some proteins. Contact residues within the phosphatidylinositol-binding pocket of $p47^{phox}$ are overlined, while those lining a second phosphatidic acid (PA) binding pocket are marked with an asterisk.

GeneBank™ accession no. of Noxo1α, Noxo1β, Noxo1γ, Noxo1δ, $p47^{phox}$, $p40^{phox}$, PLD1 are NM_144603, NM_172167, NM_172168, AY191359, NM_000265, NM_000631, NM_002662, respectively. FASTA™ accession no. of Bem1 and Vam7p are NP_009759 and NP_011303, respectively.

Fig. 2

Subcellular localization of Noxo1(PX)-GFP and Noxo1-GFP in two tranfected cell models. A, Noxo1α(PX)-GFP and Noxo1α-GFP are localized on intracellular vesicles or in large cytoplasmic aggregates, but not on the plasma membrane in HEK293 cells. Nuclei are stained (blue) using Hoechst 33258. Noxo1β(PX)-GFP and Noxo1β-GFP are localized predominately along the plasma membrane in HEK293 cells. Noxo1γ(PX)-GFP and Noxo1γ-GFP localize in the nucleus and weakly along the plasma membrane, particularly Noxo1γ(PX)-GFP. Noxo1δ(PX)-GFP and Noxo1δ-GFP show localization patterns similar to that of Noxo1α, and no nuclear localization, as observed with Noxo1γ(PX)-GFP and Noxo1γ-GFP. Bar: 10 μm B, Noxo1α(PX)-GFP and Noxo1α-GFP are detected at low levels on the plasma membrane (arrows), as well as on intracellular vesicles of COS-7 cells. Noxo1β(PX)-GFP and Noxo1β-GFP are localized on the plasma membrane. Noxo1γ(PX)-GFP and Noxo1γ-GFP are again localized on the plasma membrane and in the nucleus of COS7 cells. Noxo1δ(PX)-GFP and Noxo1δ-GFP

show localization patterns similar to Noxo1α and no significant nuclear association. Plasma membrane localization of Noxo1δ(PX)-GFP and Noxo1δ-GFP is less than that seen with Noxo1α(PX)-GFP and Noxo1α-GFP. C, The conserved Arg 40 mutation apparently disrupts the association of Noxo1β-GFP with the plasma membrane (arrow) in HEK293 cells. Bar: 10 μm D, Western blotting confirms comparable levels and stability of all four Noxo1 fusion proteins in HEK293 and COS-7 cells. Comparable sample loading is confirmed by β-tubulin immunoblotting. Results are representative of those obtained in three separate experiments

Fig. 3

Activation of Nox1 by Noxo1α, Noxo1β, and Noxo1γ in three transfected cell models.
In HEK293 (A) and in CHO-K1 (C) cells, Nox1 activity is efficiently supported by Noxo1β, moderately by Noxo1γ, and poorly by Noxo1α. In contrast, in COS-7 cells (C) Nox1 activity is supported at similar levels by all three Noxo1 isoforms. The enhancing effects of PMA are greater in HEK293 and CHO-K1 cell models than the COS-7 cell model. Dominant negative effects of $p22^{phox}$(P156Q) are seen with all three isoforms in all cell models, but is most apparent with Noxo1α in all cell models. D, Nox1 activity reconstituted by Noxo1β in the CHO cell model is a fraction of that observed in the other two models. Data are from at least three independent experiments

Fig. 4

Phospholipid binding of PX domain of Noxo1 isoforms.

A, SDS-PAGE analysis of GST-Noxo1α reveals poor yield of the intact 43 kDa fusion protein and a major GST degradation product (25kDa). Intact GST-Noxo1β(PX) and GST-Noxo1γ(PX) are detected at expected molecular weights (~43 kDa). B, GST-Noxo1β binds to PtdIns-(3)P, PtdIns-(4)P, and PtdIns-(5)P, PtdIns-(3,5)P_2, and phosphatidic acid (PA). GST-Noxo1γ shows almost the same binding pattern, while GST shows no lipid binding. LPA, Lysophosphatidic acid; LPC, Lysophosphatidylcholine; PE, phosphatidylethanolamine; PS, phosphatidylcholine; S1P, sphingosine 1-phosphate; PS, phosphatidylserine Results shown were similar in three independent experiments.

Fig. 5

Tissue-specific expression patterns of Noxo1 isoform mRNAs.

A, Noxo1 mRNAs (arrow) are detected by RT-PCR using single-strand cDNA templates prepared from colon, testis (test), liver, and pancreas (panc). Noxo1 mRNA is faintly detected in pancreas. M, marker; cont, control reaction without cDNA template. Noxo1β and Noxo1γ cDNAs are detected from all tissues, however, Noxo1α is detected in testis and liver, and Noxo1δ

is detected only in liver. C, Alternatively-spliced Noxo1-GFP isoforms show distinct subcellular distribution patterns in pancreatic (PANC-1) and testis (TM3) epithelial cell lines. Noxo1α is predominately vesicular (arrows: the plasma membrane), Noxo1β associates with the plasma membrane, and Noxo1γ is both in nuclei and on the plasma membrane. Bar: 10 μm.

Fig. 6

Nox1-dependent, but Noxo1-independent, targeting of endogenous $p22^{phox}$ to the plasma membrane.

A, Immunofluorescence imaging of endogenous and transfected $p22^{phox}$ in HEK293 cells, showing a reticular cytoplasmic and peri-nuclear membrane (*arrows*) staining patterns. Transfection of Nox1 results in a redistribution of endogenous $p22^{phox}$ to the plasma membrane. *, control cells not transfected with Nox1 show much weaker staining of endogenous $p22^{phox}$, primarily in a reticular cytoplasmic pattern. B, Transfection of Noxo1(α, β, or γ)-GFP shows no redistribution of endogenous $p22^{phox}$. C, Western blotting shows increased $p22^{phox}$ levels in Nox1-transfected, but not in mock or Noxo1β-transfected cells. Comparable protein loading is confirmed by β-tubulin immunoblotting. Similar results were obtained in three independent experiments.

Figure 1

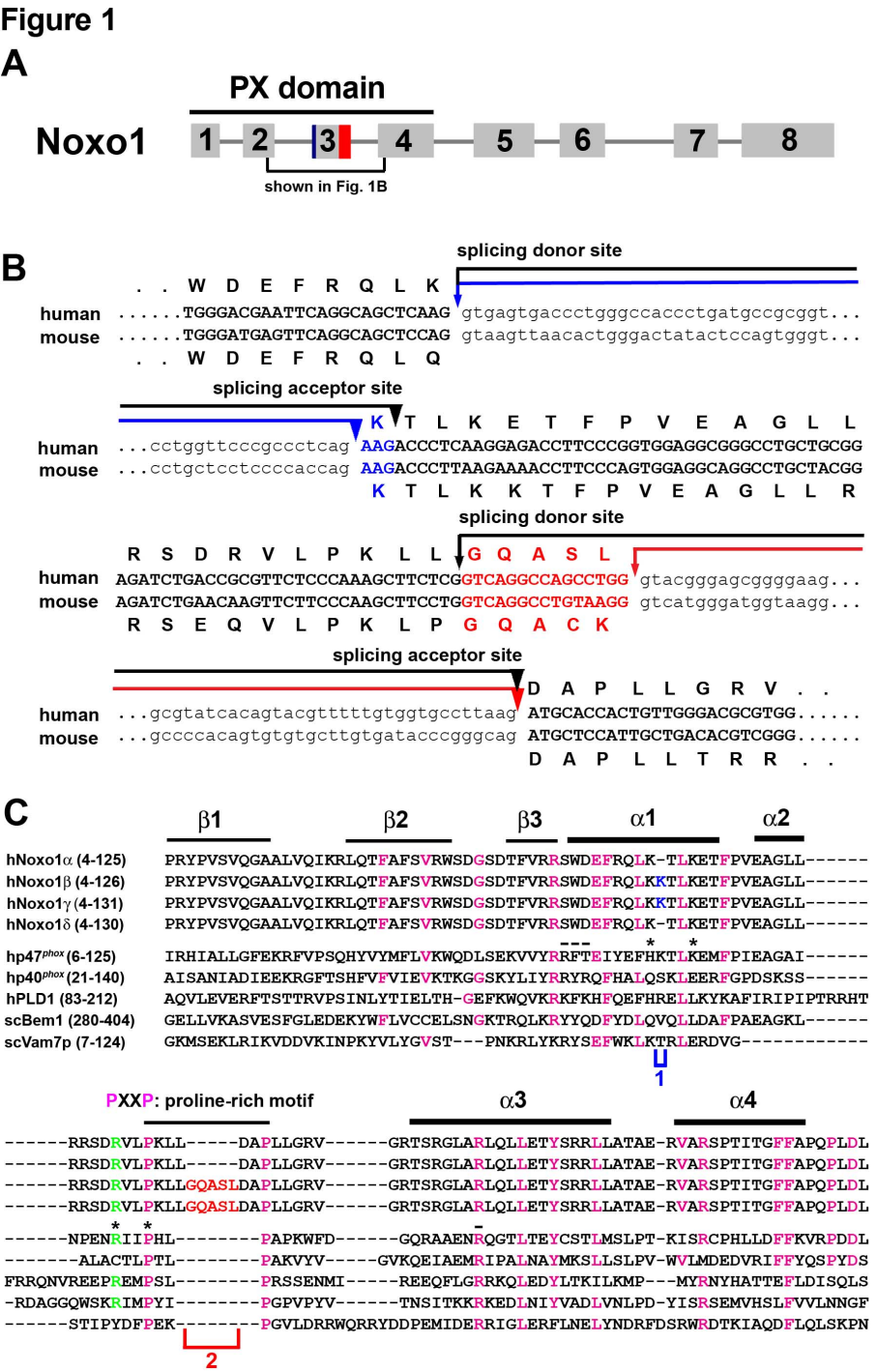
A
PX domain
Noxo1
1
2
3
4
5
6
7
8
shown in Fig. 1B
B
splicing donor site
. . W D E F R Q L K
human ......TGGGACGAATTCAGGCAGCTCAAG gtgagtgaccctgggccaccctgatgccgcggt...
mouse ......TGGGATGAGTTCAGGCAGCTCCAG gtaagttaacactgggactatactccagtgggt...
. . W D E F R Q L Q
splicing acceptor site
K T L K E T F P V E A G L L
human ...cctggttcccgccctcag AAGACCCTCAAGGAGACCTTCCCGGTGGAGGCGGGCCTGCTGCGG
mouse ...cctgctcctccccaccag AAGACCCTTAAGAAAACCTTCCCAGTGGAGGCAGGCCTGCTACGG
K T L K K T F P V E A G L L R
splicing donor site
R S D R V L P K L L G Q A S L
human AGATCTGACCGCGTTCTCCCAAAGCTTCTCGGTCAGGCCAGCCTGG gtacgggagcggggaag...
mouse AGATCTGAACAAGTTCTTCCCAAGCTTCCTGGTCAGGCCTGTAAGG gtcatgggatggtaagg...
R S E Q V L P K L P G Q A C K
splicing acceptor site
D A P L L G R V . .
human ...gcgtatcacagtacgtttttgtggtgccttaag ATGCACCACTGTTGGGACGCGTGG.....
mouse ...gccccacagtgtgtgcttgtgataccgggcag ATGCTCCATTGCTGACACGTCGGG.....
D A P L L T R R . .
C
β1
β2
β3
α1
α2
hNoxo1α (4-125) PRYPVSVQGAALVQIKRLQTFAFSVRWSDGSDTFVRRSWDEFRQLK-TLKETFPVEAGLL------
hNoxo1β (4-126) PRYPVSVQGAALVQIKRLQTFAFSVRWSDGSDTFVRRSWDEFRQLKKTLKETFPVEAGLL------
hNoxo1γ (4-131) PRYPVSVQGAALVQIKRLQTFAFSVRWSDGSDTFVRRSWDEFRQLKKTLKETFPVEAGLL------
hNoxo1δ (4-130) PRYPVSVQGAALVQIKRLQTFAFSVRWSDGSDTFVRRSWDEFRQLK-TLKETFPVEAGLL------
hp47phox (6-125) IRHIALLGFEKRFVPSQHYVYMFLVKWQDLSEKVVYRRFTEIYEFHKTLKEMFPIEAGAI------
hp40phox (21-140) AISANIADIEEKRGFTSHFVFVIEVKTKGGSKYLIYRRYRQFHALQSKLEERFGPDSKSS------
hPLD1 (83-212) AQVLEVERFTSTTRVPSINLYTIELTH-GEFKWQVKRKFKHFQEFHRELLKYKAFIRIPIPTRRHT
scBem1 (280-404) GELLVKASVESFGLEDEKYWFLVCCELSNGKTRQLKRYYQDFYDLQVQLLDAFPAEAGKL------
scVam7p (7-124) GKMSEKLRIKVDDVKINPKYVLYGVST---PNKRLYKRYSEFWKLKTRLERDVG----------
1
PXXP: proline-rich motif
α3
α4
------RRSDRVLPKLL-----DAPLLGRV------GRTSRGLARLQLLETYSRRLLATAE-RVARSPTITGFFAPQPLDL
------RRSDRVLPKLL-----DAPLLGRV------GRTSRGLARLQLLETYSRRLLATAE-RVARSPTITGFFAPQPLDL
------RRSDRVLPKLLGQASLDAPLLGRV------GRTSRGLARLQLLETYSRRLLATAE-RVARSPTITGFFAPQPLDL
------RRSDRVLPKLLGQASLDAPLLGRV------GRTSRGLARLQLLETYSRRLLATAE-RVARSPTITGFFAPQPLDL
------NPENRIIPHL--------PAPKWFD------GQRAAENRQGTLTEYCSTLMSLPT-KISRCPHLLDFFKVRPDDL
------ALACTLPTL--------PAKVYV-----GVKQEIAEMRIPALNAYMKSLLSLPV-WVLMDEDVRIFFYQSPYDS
FRRQNVREEPREMPSL--------PRSSENMI-----REEQFLGRRKQLEDYLTKILKMP---MYRNYHATTEFLDISQLS
-RDAGGQWSKRIMPYI--------PGPVPYV------TNSITKKRKEDLNIYVADLVNLPD-YISRSEMVHSLFVVLNNGF
------STIPYDFPEK--------PGVLDRRWQRRYDDPEMIDERRIGLERFLNELYNDRFDSRWRDTKIAQDFLQLSKPN
2

Figure 2

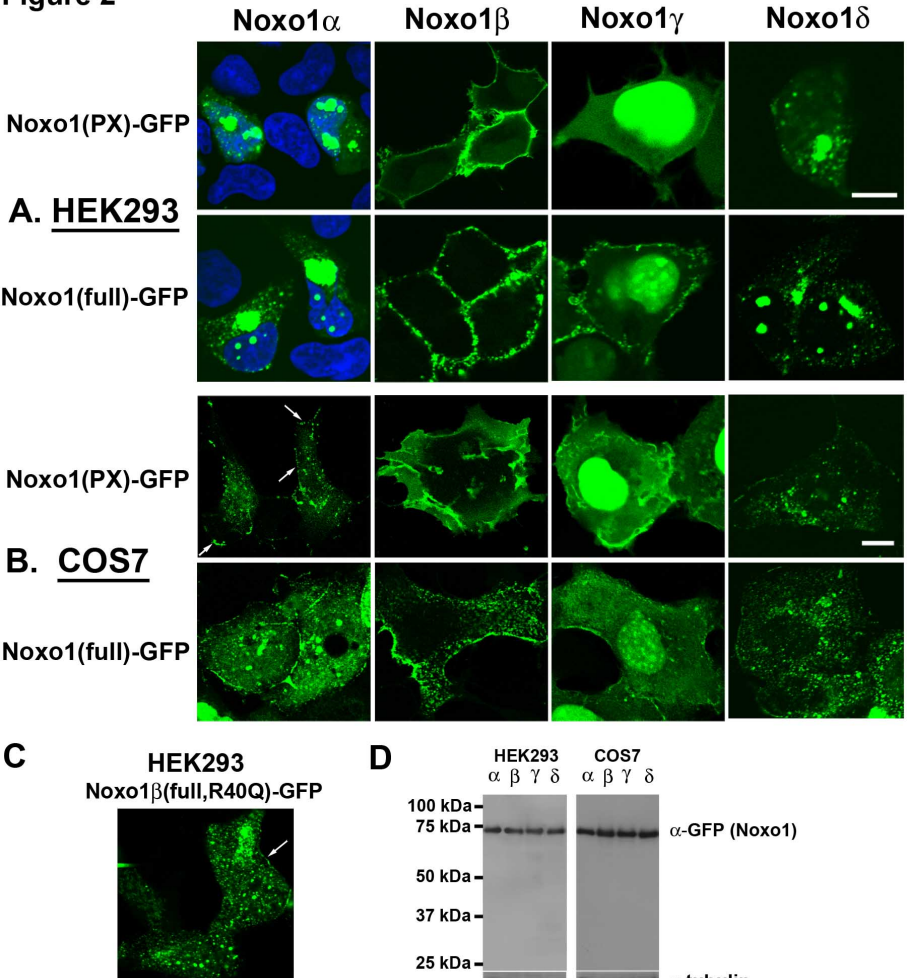
Noxo1α
Noxo1β
Noxo1γ
Noxo1δ
Noxo1(PX)-GFP
A. HEK293
Noxo1(full)-GFP
Noxo1(PX)-GFP
B. COS7
Noxo1(full)-GFP
C
HEK293
Noxo1β(full,R40Q)-GFP
D
HEK293
COS7
α β γ δ α β γ δ
100 kDa
75 kDa
50 kDa
37 kDa
25 kDa
α-GFP (Noxo1)
α-tubulin

Figure 3

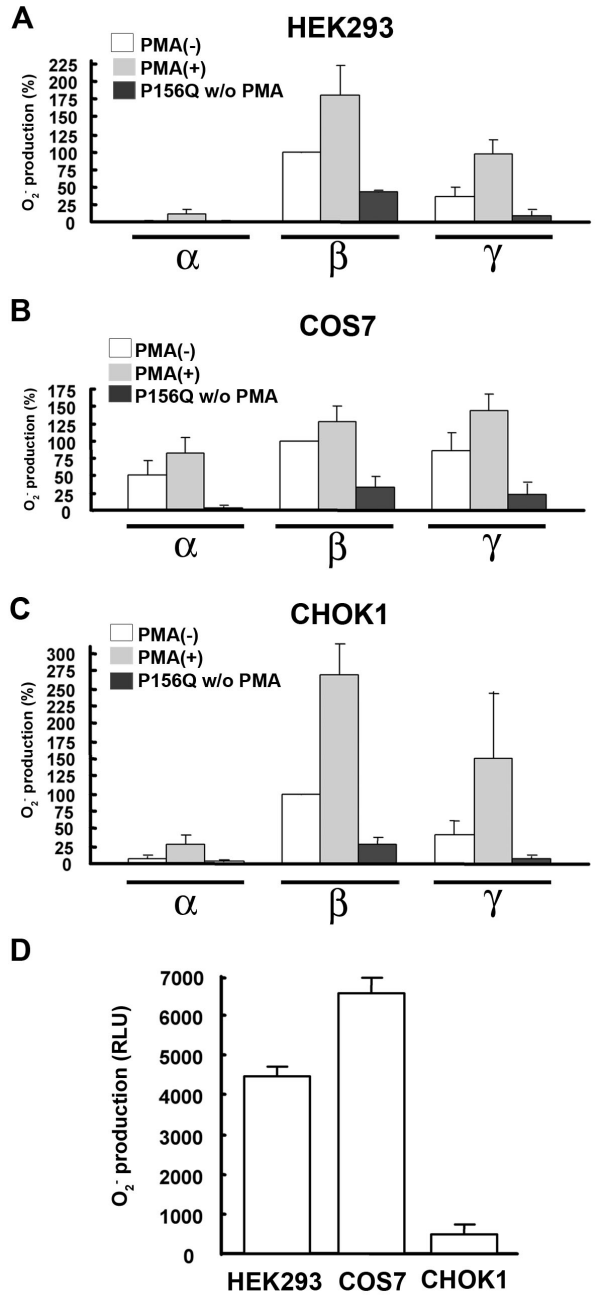
A
HEK293
PMA(-)
PMA(+)
P156Q w/o PMA
O2- production (%)
225
200
175
150
125
100
75
50
25
0
α
β
γ
B
COS7
PMA(-)
PMA(+)
P156Q w/o PMA
O2- production (%)
175
150
125
100
75
50
25
0
α
β
γ
C
CHOK1
PMA(-)
PMA(+)
P156Q w/o PMA
O2- production (%)
300
275
250
225
200
175
150
125
100
75
50
25
0
α
β
γ
D
O2- production (RLU)
7000
6000
5000
4000
3000
2000
1000
0
HEK293
COS7
CHOK1

Figure 4

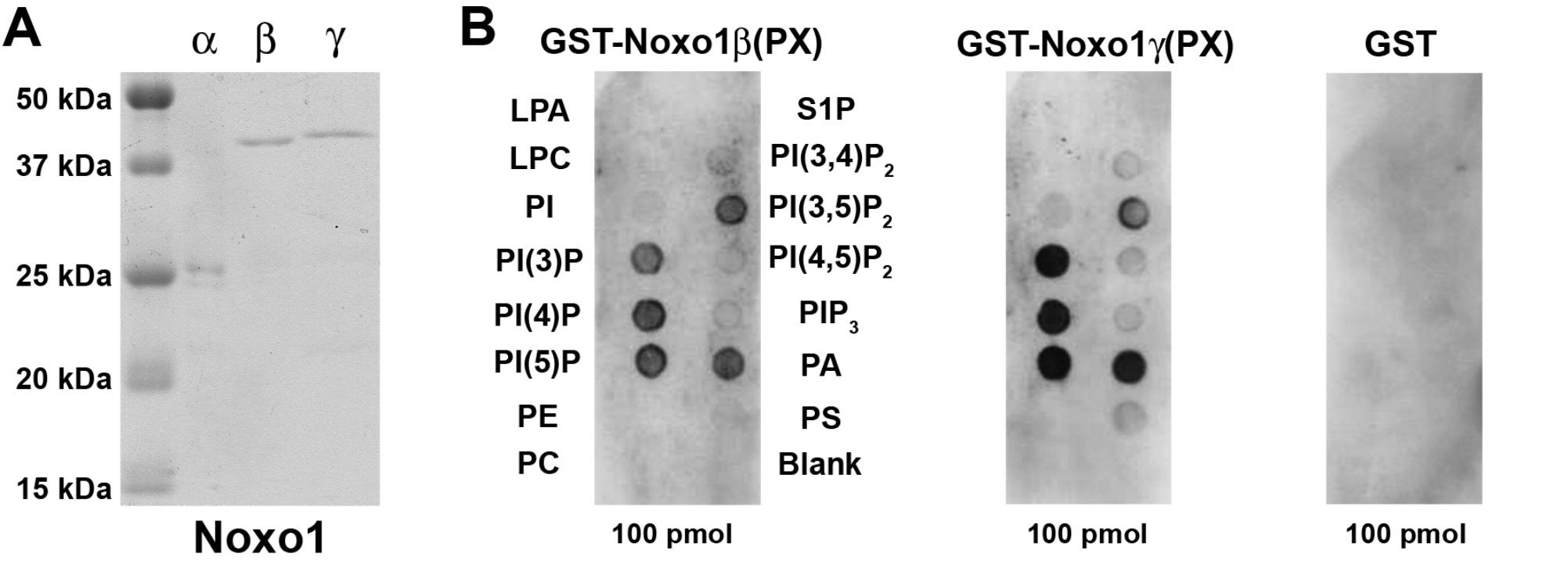
A
α
β
γ
50 kDa
37 kDa
25 kDa
20 kDa
15 kDa
Noxo1
B
GST-Noxo1β(PX)
GST-Noxo1γ(PX)
GST
LPA
LPC
PI
PI(3)P
PI(4)P
PI(5)P
PE
PC
S1P
PI(3,4)P2
PI(3,5)P2
PI(4,5)P2
PIP3
PA
PS
Blank
100 pmol
100 pmol
100 pmol

Figure 5

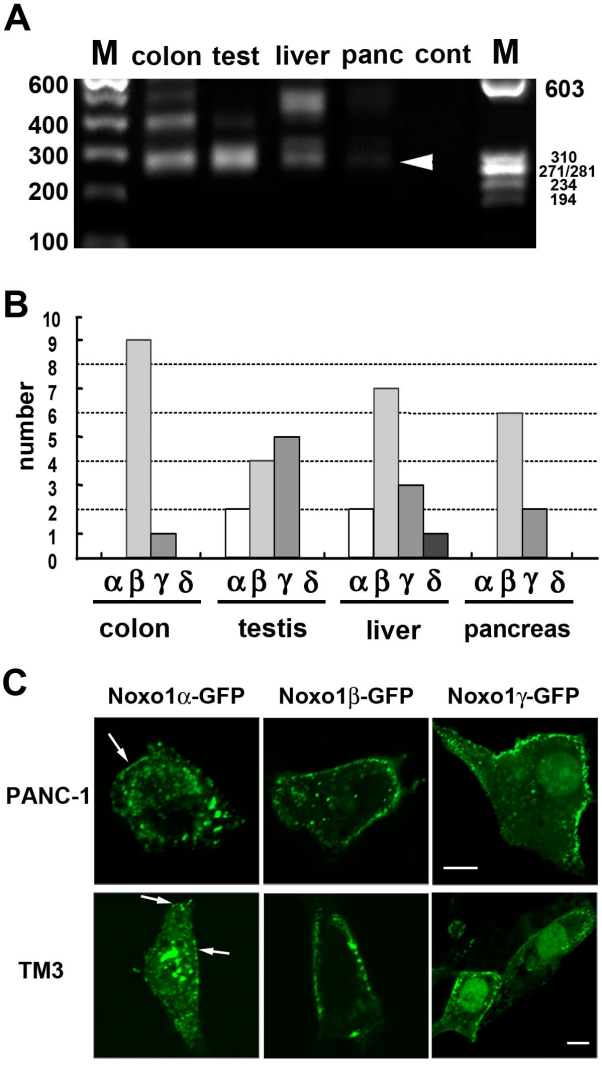
A
M colon test liver panc cont M
600
400
300
200
100
603
310
271/281
234
194
B
number
10
9
8
7
6
5
4
3
2
1
0
α β γ δ
α β γ δ
α β γ δ
α β γ δ
colon
testis
liver
pancreas
C
Noxo1α-GFP
Noxo1β-GFP
Noxo1γ-GFP
PANC-1
TM3

Figure 6

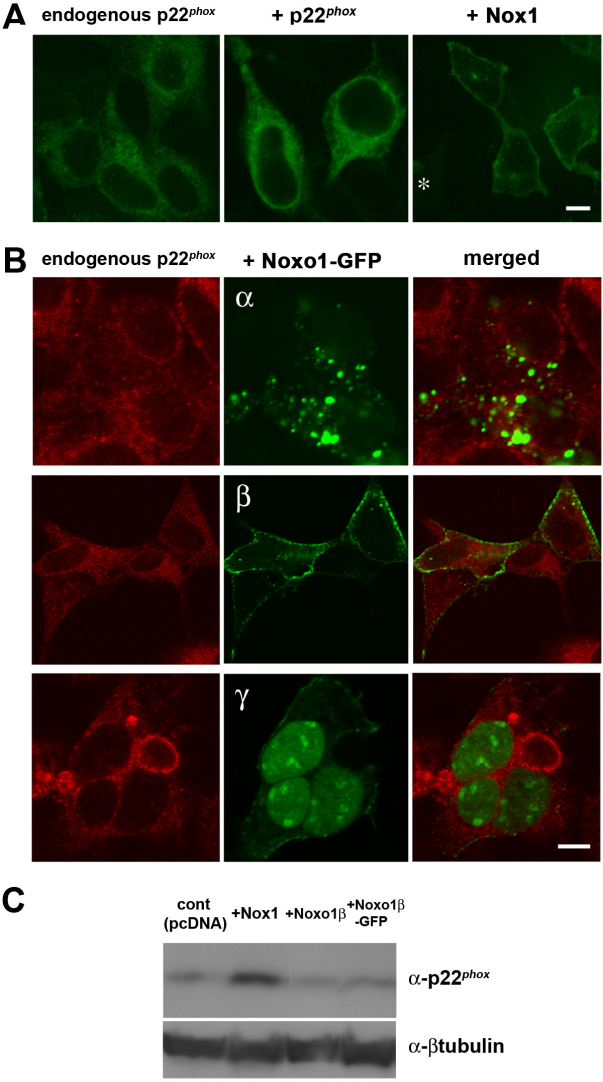
A
endogenous p22phox
+ p22phox
+ Nox1
*
B
endogenous p22phox
+ Noxo1-GFP
merged
α
β
γ
C
cont (pcDNA)
+Nox1
+Noxo1β
+Noxo1β -GFP
α-p22phox
α-βtubulin